Received: 17 April 2020 | Revised: 10 July 2020 | Accepted: 23 July 2020

DOI: 10.1002/jrs.5965

SPECIAL ISSUE - RESEARCH ARTICLE

Journal of RAMAN SPECTROSCOPY WILEY

Bio-probing with nonresonant surface-enhanced hyper-Raman scattering excited at 1,550 nm

Zsuzsanna Heiner[1,2] | **Fani Madzharova**[1] | **Vesna Živanović**[1,2] | **Janina Kneipp**[1,2]

[1]Department of Chemistry, Humboldt-Universität zu Berlin, Brook-Taylor-Str. 2, Berlin, 12489, Germany

[2]School of Analytical Sciences Adlershof, Humboldt-Universität zu Berlin, Albert-Einstein-Str. 6-9, Berlin, 12489, Germany

Correspondence
Janina Kneipp, Department of Chemistry, Humboldt-Universität zu Berlin, Brook-Taylor-Str. 2, 12489 Berlin, Germany.
Email: janina.kneipp@chemie.hu-berlin.de

Funding information
Fonds der Chemischen Industrie; Deutsche Forschungsgemeinschaft, Grant/Award Number: GSC 1013; FP7 Ideas: European Research Council, Grant/Award Number: 259432

Abstract

The two-photon excited process of surface-enhanced hyper-Raman scattering (SEHRS) provides advantages for studies of complex biological samples, yet suitable SEHRS nanoprobes and labels, as well as experimental conditions, must be established. Here, SEHRS spectra of the four reporter molecules (2-naphthalenethiol [2-NAT], *para*-aminothiophenol (*p*ATP), *para*-nitrothiophenol (*p*NTP), and crystal violet), as well as the two antidepressant drugs (desipramine and imipramine) were obtained at an excitation wavelength of 1,550 nm using different citrate-stabilized gold nanoparticles and silver nanoparticles, and under conditions that permit experiments with living cultured cells. As the results suggest, the short-wave infrared laser excitation and the hyper-Raman scattered light (corresponding to wavelengths > 775 nm) match the plasmonic properties of the employed gold and silver nanoaggregates, as well as the requirements regarding the viability of the cells. The two-photon excited spectra of three types of SEHRS labels containing 2-NAT as reporter inside macrophage cells show that molecules in the cellular environment can also be observed. The possibility to use short-wave infrared excitation with gold nanostructures has important implications for the utilization of SEHRS in bio-probing.

KEYWORDS

gold nanoparticles, short-wave infrared, silver nanoparticles, surface-enhanced hyper-Raman scattering (SEHRS)

1 | INTRODUCTION

The vibrational characterization of bioorganic samples has benefitted significantly from the introduction of molecular labels and probes. By exploiting surface-enhanced Raman scattering (SERS),[1–3] SERS labels or labeled probes,[4] consisting of plasmonic nanoparticles together with a reporter molecule, can be used to mark biological structures in cells,[5,6] antibodies,[7,8] and tissues in whole animals.[9,10] The biological structures are highlighted owing to the strong SERS signals that are obtained from the reporter molecule. The reporter molecule can also be chosen to be an indicator of changes in the biological environment of a SERS labeled probe, for example, changes in pH[11] or the presence of reactive oxygen species,[12] or changes in temperature.[13] Reporters can also be multifunctional; as important examples, drugs that are delivered by gold nanoparticles

can be followed by their own SERS spectrum,[14] and their interaction with the biological environment can be monitored.[15]

Apart from using the one-photon excited SERS, also the two-photon excited process of surface-enhanced hyper-Raman scattering (SEHRS)[16–18] can be utilized to excite plasmonic probes in cells and tissues[19] and to generate combined SERS/SEHRS probes of pH for biological probing.[20–22] Although the scattering probabilities for the incoherent SEHRS process are lower than those of SERS or of coherent two-photon excited Raman processes (e.g., CARS or SRS), the SEHRS cross section is similar to or even higher than the cross sections of two-photon fluorescent probes.[19] The high cross sections suggest the applicability[19] of SEHRS vibrational labels using SEHRS for microscopic probing and imaging of biological samples.[21,23] This is extremely attractive, because of the different selection rules of hyper-Raman scattering and SEHRS in particular,[24–26] additional, complementary information from vibrational probes can be gained for fingerprinting and imaging. Moreover, because of the special sensitivity of SEHRS to small changes in surface potential and adsorbate orientation,[18,27,28] small changes to reporter molecules may be detected,[29,30] thereby improving chemical probing. While the hyper-Raman scattering light lies in the ultraviolet range when the sample is excited in the visible,[31] excitation in the near-infrared region from 800 to 1,000 nm, generating hyper-Raman light in the visible region, was shown to be beneficial, especially with respect to exploiting the local fields of plasmonic nanostructures in SEHRS.[32–34] SEHRS of dyes and thiolated molecules excited at wavelengths around 1,550 and 1,800 nm using silver nanoparticles was shown to be feasible.[35,36] Considering the benefits of excitation in the near-infrared for biological samples, including improved penetration depth and reduced (one-photon) autofluorescence, as well as reduced photochemical damage due to almost complete absence of electronic resonances in the probed molecules, such long wavelengths for SEHRS experiments would be very useful. As specific advantage, both the excitation wavelength and the hyper-Raman light lie in the near-infrared transparent spectral region of biological samples.

Here, we report the nonresonant SEHRS spectra of four molecules that can serve as efficient reporters in SEHRS and SERS of biological samples, as well as of the two tricyclic antidepressants imipramine and desipramine in their interaction with gold and silver nanoparticles, excited with 1,550 nm. The wavelengths of 1,550 nm and of the hyper-Raman light of >775 nm match both the typical plasmon resonances of aggregates of the nanoparticles and the requirements of the biological samples. Mapping measurements of a reporter were obtained from living macrophage cells that contained the SEHRS nanoprobes comprising silver and gold nanoparticles, respectively, and the possibility to observe cellular constituents in the SEHRS spectra is demonstrated. The results represent a further step towards more biocompatible SEHRS probing and its applications in biotechnology and theranostics.

2 | MATERIALS AND METHODS

2.1 | Preparation of SEHRS reporters and nanoprobes

Gold(III) chloride trihydrate ($HAuCl_4 \cdot 3H_2O$, 99.9% trace metals basis), silver nitrate (99.9999% trace metals basis), *para*-aminothiophenol (*p*ATP), *para*-nitrothiophenol (*p*NTP), 2-naphthalenethiol (2-NAT), desipramine hydrochloride (>98%), and imipramine hydrochloride (>99%) were purchased from Sigma-Aldrich. Trisodium citrate dihydrate (99%) was obtained from Th. Geyer, and sodium chloride and crystal violet (CV) were purchased from J. T. Baker. All solutions were prepared using Milli-Q water (USF Elga Purelab Plus purification system).

Three different types of colloidal particles were prepared. Gold nanoparticles with two sizes were produced by reduction of gold(III) chloride with sodium citrate following slightly different protocols. Gold nanoparticles of a size of ~50 nm (termed Au50 in the following discussions) with an absorbance maximum at 544 nm were prepared following the procedure by Frens.[37] They were used for the experiments with the reporter molecules and the drugs. Gold nanoparticles with a size of ~30 nm (termed Au30) and an absorbance maximum at 529 nm were produced by the Lee and Meisel protocol.[38] Citrate-reduced silver nanoparticles, termed Ag, with an absorbance maximum at 430 nm were also produced by the Lee and Meisel protocol.[38] The size of all nanoparticles was estimated based on the transmission electron micrographs,[34,39] and the concentration of the nanoparticles was 3×10^{-10} M for the Au30, 9×10^{-11} M for the Au50, and 2×10^{-11} M for the Ag nanoparticles.

For the SEHRS experiments with *p*ATP, *p*NTP, 2-NAT, CV, desipramine, and imipramine, the 50-nm gold and silver were mixed with NaCl solution, which results in broadening of the plasmon band, indicating formation of nanoaggregates as shown previously for this type of nanoparticles.[39] Finally, the respective molecule solution was added to obtain the desired concentration (stated in the captions of Figures 1-3 for each sample).

For experiments with living cells, 2-NAT-containing SEHRS labels were prepared by mixing the three types of preaggregated nanoparticles (Ag, Au30, and Au50) with 2-NAT at a concentration of 10^{-6} M.

2.2 | Cell culture and incubation with SEHRS labels

Swiss albino mouse macrophages (cell line J774) (DSMZ, Braunschweig, Germany) were cultured in Dulbecco's modified Eagle medium (DMEM) supplemented with 10% fetal calf serum (FCS) and 1% ZellShield™ (Biochrom AG, Berlin, Germany) under standard conditions. For the SEHRS experiments, the cells were grown as a monolayer on sterile cover slips (Thermo Fisher Scientific, Schwerte, Germany) in a six-well plate and incubated with a mixture of 120 µl of SEHRS label and 880 µl of culture medium for 3, 5, and 7 h, respectively. After incubation, the cells were washed with phosphate-buffered saline (PBS) several times, and they were kept in fresh PBS during the SEHRS measurement.

Both before and after the Raman experiments, bright-field microscopic images were taken. No detachment or changes in shape of the investigated cells were observed, permitting the conclusion that the experimental conditions do not disturb their viability. In XTT tests performed previously,[5] it was confirmed that for the incubation time and concentration of nanoparticles and 2-NAT reporter molecule, no toxicity occurred. In the SEHRS mapping experiments with the cells, five to 10 cells for each of the four incubation times with three different SEHRS labels (Ag, Au30, and Au50) yielded data sets from 92 cells in total. The number of mapping points per cell was typically between 15 and 25.

2.3 | SEHRS spectroscopy and imaging experiments

All SEHRS spectra were obtained with a home-built microspectrometer[29] using a 1,550-nm laser, producing 35-ps pulses at a repetition rate of 76 MHz (Katana HP, Onefive) for excitation. Liquid samples were placed in microcontainers, and the excitation light was focused onto the samples through a 15× Schwarzschild objective with a numerical aperture of 0.3 in epi-illumination geometry. The cell measurements were conducted by focusing the laser light with a 60× water immersion objective (NA 1.2) and raster scanning various small areas with a step size of 2 µm and an acquisition time of 60 s per spectrum while keeping the laser excitation power below 2 mW, corresponding to maximum photon flux densities of 4.5×10^{26} photons·cm^{-2}·s^{-1}. The hyper-Raman scattered light was detected by a single-stage Czerny–Turner spectrograph equipped with a liquid nitrogen cooled CCD. The spectral resolution was 3–4 cm^{-1} in the full spectral range. For comparison, SEHRS spectra of liquid samples were also obtained at 1,064-nm (7 ps, 76 MHz) and 830-nm (5 ps, 80 MHz) excitation (see Supporting Information). Excitation intensities and accumulation times used for each sample are stated in the captions.

The SEHRS spectra of the liquid samples were wavenumber calibrated, de-spiked, and background corrected using an automated background correction algorithm.[40] The spectra collected in from the living cells were wavenumber calibrated and de-spiked.

3 | RESULTS AND DISCUSSION

3.1 | SEHRS spectra of reporter molecules excited at 1,550 nm

SEHRS spectra of the reporter molecules CV, 2-NAT, *p*ATP, and *p*NTP were obtained at 1,550-nm excitation in the presence of gold and silver nanoparticles, respectively. The spectra of CV on silver (Figure 1a) and gold (Figure 1b) show characteristic bands at 1,618, 1,587, 1,367, 1,297, and 1,176 cm^{-1} (see Table 1 for band assignments) and are in good agreement with previously published data using 1,570-nm excitation[36] and also with other SEHRS spectra with small or no molecular resonance contribution.[32] Comparing the off-resonant CV spectra at 1,550 nm with spectra obtained at 1,064 and 830 nm (Supplementary Information Figure S1A, S1B and S1C), the intensity of the in-plane ring stretching at 1,587 cm^{-1} is clearly decreased relative to the *N*-phenyl stretching at 1,367 cm^{-1}, which we attribute to different two-photon resonant contributions that are present when using 1,064 or 830-nm excitation.[32,36,50]

The SEHRS spectra of 2-NAT with 50-nm gold (Figure 1c) and silver nanoparticles (Figure 1d) at 1,550 nm is very similar and show strong contributions from the ring stretching modes at 1,615, 1,570, and 1,376 cm^{-1} as well as from the CH bending at 1,064 cm^{-1} (see Table 1).[41] They are in agreement with previously reported spectra of the molecule excited at 1,064 nm[21] and also similar to the SEHRS spectra excited at 830 nm (compare Figure S2A with S2B and S2C). Small changes in relative intensities, as that of the ring stretching mode at 1,615 cm^{-1} (Figure S2), can be the result of changed electronic resonance conditions in place for the covalently interacting 2-NAT species[51] that influence the enhancement of these vibrational modes.

Comparison of the spectra obtained with the silver nanoparticles (Figure 1a,c) shows that the overall signal of 2-NAT is about one order of magnitude stronger than that of CV, which is in the same order of magnitude as the difference in the applied concentration and suggests a similar enhancement for both molecules.

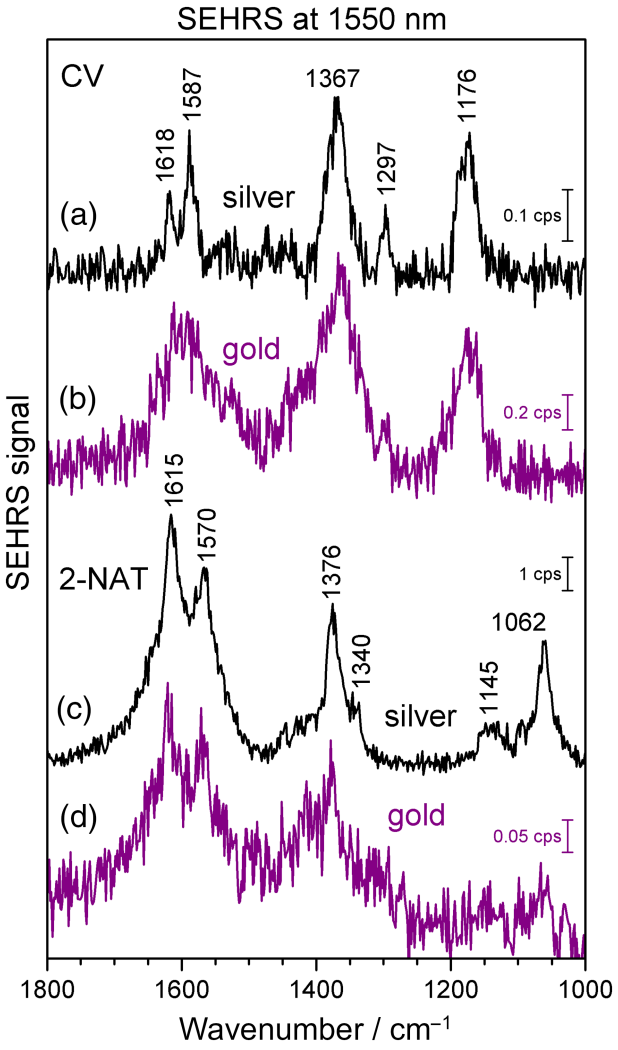

FIGURE 1 Surface-enhanced hyper-Raman scattering (SEHRS) spectra of (a, b) crystal violet (CV) and (c, d) 2-naphthalenethiol (2-NAT) obtained with silver (a, c) and 50-nm gold (b, d) nanoparticles. Excitation, 1,550 nm; laser peak intensity, 5×10^7 W·cm^{-2}; acquisition time, 5 min (a), 3 min (b), 1 min (c), and 6 min (d). Concentration, 8×10^{-7} M (a, b) and 8×10^{-6} M (c, d)

TABLE 1 Raman shift values in the 1,550 nm-excited surface-enhanced hyper-Raman scattering (SEHRS) spectra of crystal violet (CV), 2-naphthalenethiol (2-NAT), *para*-aminothiophenol (*p*ATP), *para*-nitrothiophenol (*p*NTP), desipramine, and imipramine and proposed band assignment based on previous work[39,41–46]

	Raman shift, cm^{-1}	Assignment
CV[44,45]	1,618	N-Ph str, CC str
	1,587	i.p. ring str
	1,367	N-Ph str
	1,297	i.p. ring bend
	1,176	i.p. CH bend (Ph)
2-NAT[41]	1,615	Ring str
	1,570	Ring str
	1,376	Ring str
	1,340	Ring str
	1,145	CH bend
	1,062	CH bend
*p*ATP[39,47]	1,582	Ring CC str, symm NH_2 bend
	1,077	CS str, i.p. C–C–C bend
*p*NTP[48,49]	1,570	Ring CC str
	1,335	Symm NO_2 str
	1,073	CS str
Desipramine[42,43]	1,297	CC str (bridge bond, 7-membered ring)
	1,157	CH rock (aromatic ring)
Imipramine[42,43]	1,294	CC str (bridge bond, 7-membered ring)
	1,160	CH rock (aromatic ring)

Abbreviations: asymm, asymmetric; bend, bending; i.p., in plane; o.o.p.,out of plane; Ph, phenyl ring; rock, rocking; str, stretching; symm, symmetric.

The SEHRS spectra of *p*ATP and *p*NTP obtained with silver nanoparticles (Figure 2a, black line, and b, black line, respectively) are qualitatively very similar to the spectra with 50-nm gold nanoparticles (Figure 2a, blue line, and b, green line). The spectra of *p*ATP (Figure 2a) display two prominent bands at 1,582 and 1,077 cm^{-1}, which are assigned to the ring C–C and C–S stretching modes, respectively (Table 1) and are also observed in the SEHRS spectra of the molecule on silver nanoparticles excited at 1,064 nm.[39] Although the SEHRS spectra of *p*NTP have not been reported so far, the assignment of these bands can be made using its well-known SERS spectrum.[48,52] The spectra of *p*NTP (Figure 2b) show contributions from the C–C and C–S bands at 1,570 and 1,073 cm^{-1} as well. They are clearly dominated by the NO_2 stretching vibration at 1,335 cm^{-1} (Table 1).

Comparing the signals in those samples that interact with the metal surface via a thiol group, that is, 2-NAT (Figure 1c,d), *p*ATP (Figure 2a), and *p*NTP (Figure 2b), we see that the signal at the same molecular concentration is one order of magnitude higher with the silver nanoparticles than with gold nanoparticles (compare the respective scale bars in Figures 1c,d and 2). In contrast, the intensity difference in the SEHRS spectra of CV using silver and 50-nm gold nanoparticles is only about a factor of 2. Based on the concentration and size of the nanoparticles and of the molecules, the available surface areas for the different types of nanoparticles were approximately the same, suggesting that the observed

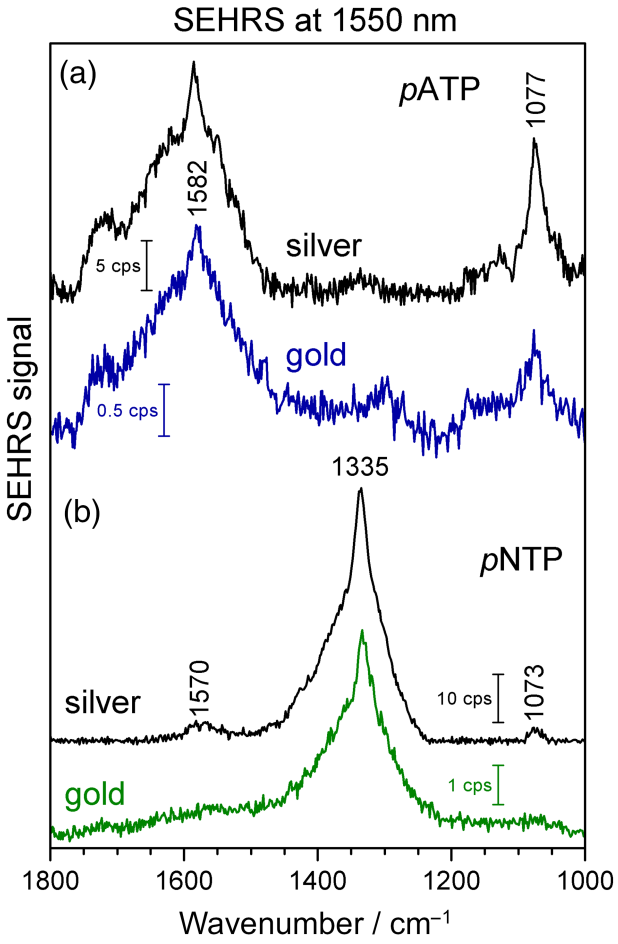

FIGURE 2 Surface-enhanced hyper-Raman scattering (SEHRS) spectra of (a) *para*-aminothiophenol (*p*ATP) and (b) *para*-nitrothiophenol (*p*NTP) obtained with silver (black lines) and gold (blue and green lines) nanoparticles. Excitation, 1,550 nm; laser peak intensity, 5×10^7 W·cm^{-2}; acquisition time, 3 min; concentration, 8×10^{-6} M

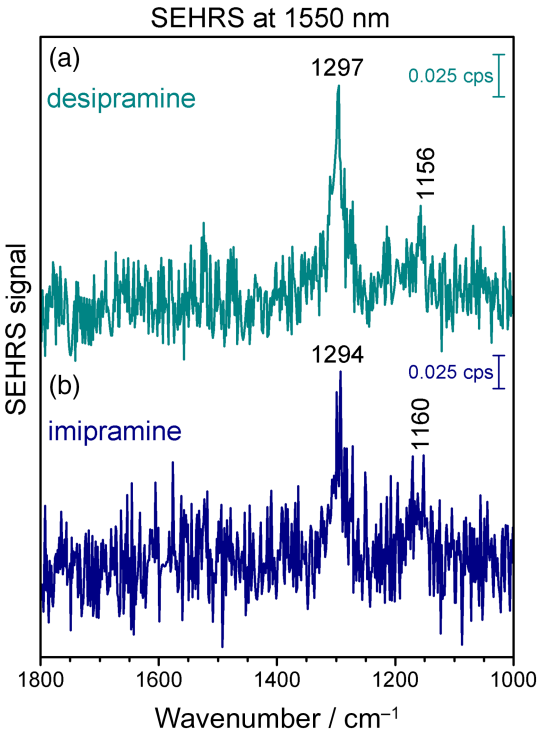

FIGURE 3 Surface-enhanced hyper-Raman scattering (SEHRS) spectra of the tricyclic antidepressants (a) desipramine and (b) imipramine obtained with gold nanoparticles. Excitation, 1,550 nm; laser peak intensity, 5×10^7 W·cm^{-2}; acquisition time, 10 min (a) and 5 min (b); concentration, 10^{-4} M

differences in signal strength originate from a different interaction of the thiolated molecules with the gold and the silver surfaces, respectively. This may, particularly, concern thermodynamic and kinetic aspects of formation of the thiol-based self-assembled monolayers on silver and gold surfaces.[53,54] Also, small variations in plasmonic properties of the nanoaggregates, known to be crucial determinants of the enhancement in SEHRS,[34] play a role at this excitation wavelength.

3.2 | SEHRS spectra of tricyclic antidepressant drugs excited at 1,550 nm

It was also possible to obtain off-resonant SEHRS spectra at 1,550 nm of the tricyclic antidepressants desipramine and imipramine using gold nanoparticles (Figure 3). The combination of these molecules with gold nanoparticles is very promising, as they constitute a system that could be used for endocytotic delivery of the drugs, which have an enzyme in the lysosomes of eukaryotic cells as target.[15] Both spectra display bands at ~1,295 and ~1,160 cm^{-1}, which could be assigned to the bridge bond C–C stretching of the seven-membered ring and the C–H in-plane bending vibration of the aromatic rings, respectively (Table 1).[42,43] These bands were observed with similar intensities relative to each other as they were also found in the 1,064 nm-excited SEHRS spectra of the drugs.[43] Some bands that were found in the spectra excited at 1,064 nm reported previously[43] were not observed in the spectra measured here (Figure 3), because of the lower sensitivity of the experiment here. This is, on the one hand, due to a different plasmonic enhancement[34] generated by nanoaggregates formed by the drug molecules[43] at this wavelength and, on the other hand, due to the overall lower signals caused by very low excitation intensity, preventing weaker bands from appearing in the spectrum. Because the observation of the tricyclic antidepressant molecules in live cells by SERS is very challenging and is mainly solved by screening of data sets with machine learning tools,[15] fast near-infrared (IR) vibrational imaging by SEHRS

could generate additional fingerprint-like data to identify spectral features of the drug molecules in cells in combined SERS and SEHRS vibrational imaging.

3.3 | SEHRS probing in living macrophage cells

The three different types of 2-NAT-containing SEHRS nanoprobes, corresponding to the different kinds of citrate-stabilized plasmonic nanoparticles, were applied in living macrophage cells; and hyper-Raman spectra were acquired from macrophages by raster scanning small areas of sizes between 60 and 100 μm^2. Figure 4 shows representative example spectra obtained from three individual cells incubated for 3 h with the SEHRS labels containing silver (Ag), 30-nm gold (Au30), and 50-nm gold (Au50) nanoparticles, respectively, and the reporter 2-NAT. All spectra clearly show the vibrational bands of 2-NAT (compare the spectra on Figure 4a,b with Figure 1c,d). Nevertheless, when comparing the vibrational bands in the spectra acquired inside and outside of the cells, additional bands can be observed from the cells at 1,426, 1,250, 1,095, and 980 cm^{-1} (Figure 4a–c, band positions shown in blue).

The weak band at 1,426 cm^{-1} could be the contribution of an in-plane C–H bending mode coupled with a ring C–C stretching and a C–S stretching mode.[41] Such a vibrational contribution was suggested by density functional theory (DFT) calculations and is also present in one-photon SERS spectra of 2-NAT obtained with silver and gold nanoparticles.[41,51]

The broad vibrational band around 1,250 cm^{-1} is unique to the SEHRS spectra from the cells with both Ag- and Au30-based SEHRS labels and can be assigned to a C–H deformation and/or C–C or C–N stretching mode. Interestingly, it is not visible in any of the SEHRS spectra obtained with 830-nm, 1,064-nm, and 1,550-nm excitation outside the cells (cf. Figure 1c,d, Figure S2), and neither was this band found in our previous SEHRS spectra obtained with silver nanoparticle-based 2-NAT SEHRS labels in the same cell line.[21] It is also absent in the SERS spectra inside and outside cells.[5,41,51,55,56] Therefore, rather than assigning this band to the reporter molecule 2-NAT, we conclude that it must come from the biomolecules of the cellular, that is, the intraendosomal environment. As an example, in previous SEHRS experiments with silver nanoparticles and aromatic amino acids, we assigned a strong vibrational band in this spectral region to the C–H bending or C–C ring stretching mode, specifically in tyrosine[57]; and also in SEHRS spectra of nucleobases, such as guanine, this mode can be quite pronounced.[58] Although the vibrational band at 1,250 cm^{-1} was not the most intense in the SEHRS spectrum of amino acids or nucleic acids when applying silver nanoparticles and exciting the spectra at 1,064 nm,[57,58] it is a prominent band in the present case. Other spectral features of these molecules, including bands in the vibrational region between 1,560 and 1,600 cm^{-1}, are probably obscured here owing to the overlapping strong 2-NAT ring stretching modes, and the overall enhancement is influenced by many factors. Therefore, we attribute the band at 1,250 cm^{-1} to amino acids, free or contained in proteins, or to nucleobases.

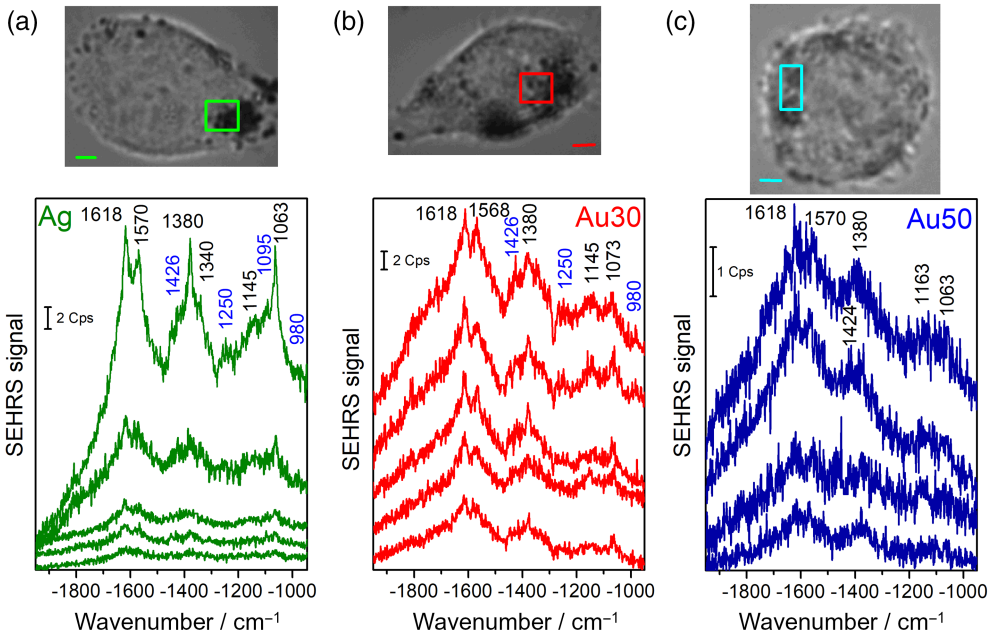

FIGURE 4 Bright-field images and representative example spectra from living J774 macrophages after 3 h of incubation with surface-enhanced hyper-Raman scattering (SEHRS) labels. The spectra were obtained using SEHRS labels with the reporter 2-NAT with (a) silver, (b) 30-nm gold, and (c) 50-nm gold nanoparticles. Mapping step size, 2 μm; scale bar, 5 μm; excitation wavelength, 1,550 nm; laser peak intensity, 7×10^7 $W \cdot cm^{-2}$ (corresponding to 1.8-mW average power); acquisition time, 60 s

The small peak at 1,095 cm^{-1} could be assigned to the combination of C–S stretching with the ring breathing mode of 2-NAT,[51] whereas the vibrational band at 980 cm^{-1} is attributed to a C–H deformation mode[41,51] or a combination of the C–S stretching with a ring breathing mode.[51] We observed no further vibrational bands from the bioorganic molecules in the culture medium or the cells, suggesting that the applied nanostructures were covered with the reporter molecule, where the chemisorption between via the thiol group and nanoparticles is expected to be strong and prohibits most other interactions under the applied experimental conditions.

Interestingly, compared with the spectra of 2-NAT obtained with the same Ag and Au50 nanoparticles outside the cells (Figure 1c,d), the signals obtained inside cells are stronger. Results from previous work on SEHRS in cells[21] indicate that the larger signal can be the result of two effects. (i) The SEHRS nanosensors could be present at high concentration, as a result of the cellular processing by endocytosis, which can yield both endosomes with high numbers of particles in individual endosomes or high numbers of particle-containing vesicles in the focal volume. (ii) The plasmonic properties inside the endolysosomes are more favorable, yielding higher electromagnetic field enhancements, for example, by the formation of nanoaggregates inside the endolysosomal vesicles. The important role of favorable conditions of plasmonic nanoaggregates in cells has been discussed extensively for SERS experiments with both gold and silver and can be monitored via soft X-ray tomography.[59,60] Specifically for the cell line used here, it was found that the macrophages contain large nanoparticle aggregates of sizes up to 460 nm after a 3-h incubation with 30-nm gold nanoparticle aggregates.[61] The uptake of silver SEHRS nanoprobes in the form of nanoparticle aggregates of a size of ~500 nm and a large difference between intracellular and extracellular SEHRS signals were also observed in a previous study, where we investigated cells of the same cell line.[21] Therefore, also here, we expect the formation of nanoparticle aggregates with sizes up to ~500 nm prior to uptake by the macrophages, and hence the presence of such aggregates in the phagolysosomes.

After a 3-h incubation time of the cells with the SEHRS labels, we obtained a weaker SEHRS signal from those labels made of the 50-nm gold nanoparticles (Figure 4f) as compared to the nanosensors based on 30-nm gold particles (Figure 4e). This effect can originate from different properties of the nanoaggregates that are formed from the different types of gold nanoparticles in the cell culture medium during delivery, as well as by varied processing inside the macrophage cells. Assuming from previous work using cryo-XT on the same type of nanoparticles, we expect the size of the nanoaggregates to increase with incubation time.[61] At the same time, it is known that the enhancement of one-photon SERS in cells critically depends on aggregate geometry[60] such as interparticle spacing and multivesicular inclusions.[62]

In order to investigate the impact of such changes in nanoaggregate optical properties in the course of processing by the cells on the SEHRS spectra, we incubated the macrophages with one type of SEHRS label (Au50) for 3, 5, and 7 h as shown in Figure 5a–c,

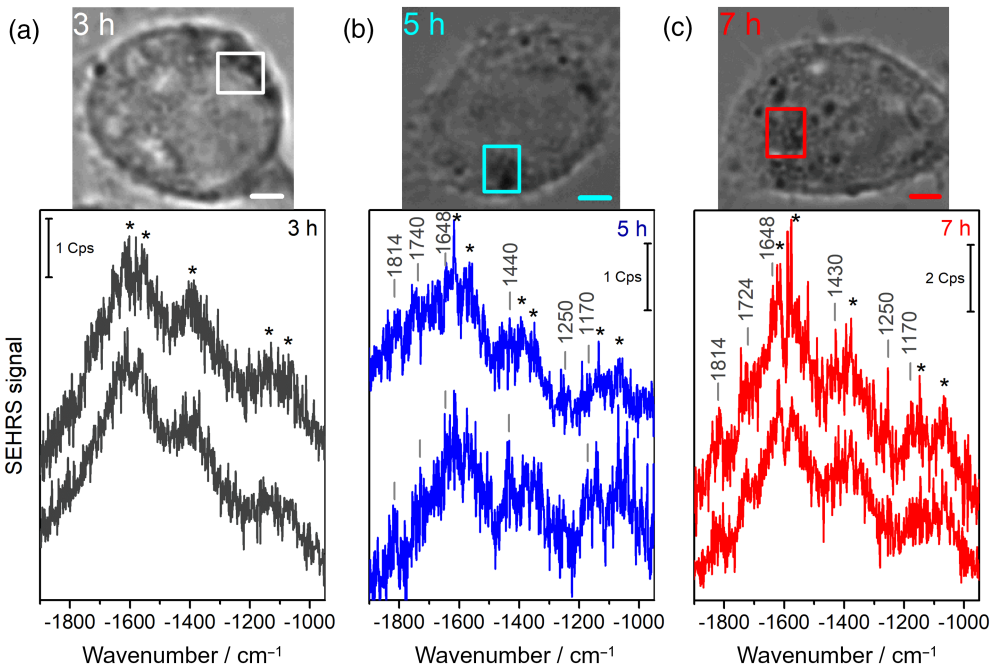

FIGURE 5 Representative spectra from living J774 macrophages containing 2-naphthalenethiol (2-NAT) surface-enhanced hyper-Raman scattering (SEHRS) labels with 50-nm gold (Au50) nanoparticles after (a) 3-, (b) 5-, and (c) 7-h incubation times and the corresponding bright-field images. The bands that correspond to the 2-NAT SEHRS labels are marked with an asterisk. Step size, 2 μm; scale bar, 5 μm; excitation wavelength, 1,550 nm; laser peak intensity, 7×10^7 $W \cdot cm^{-2}$ (corresponding to 1.8-mW average power); acquisition time, 60 s

respectively. Despite the relatively low signal-to-noise ratio in these spectra, we observe new vibrational bands in the region around 1,700 and 1,820 cm^{-1} when incubation time is increased from 3 to 5 and 7 h (Figure 5b,c). Already after 5 h of incubation (Figure 5b), small vibrational bands appeared at ~1,814 and in the region 1,720–1,740 cm^{-1}. None of them can be assigned to the reporter molecule. The peak at a center of 1,814 cm^{-1} can be assigned to an overtone or a combination mode as discussed earlier,[19] whereas the vibrational band at 1,720–1,740 cm^{-1} is associated with C═O stretching vibrations of esters from intracellular biomolecules, such as membrane lipids, including triacylglycerols and cholesterol or its derivatives, or proteins.[63–66] These bands remain present in the spectra after a 7-h incubation time as well (Figure 5c). Additional vibrational bands are observed after 5 and 7 h of incubation around 1,648, 1,440, and 1,170 cm^{-1} (Figure 5b,c) and originate from C═O/C═C stretching, NH deformation, CH_2 and/or CH_3 scissoring, and C–C stretching, respectively, owing to lipids and proteins as well.[63,64,67] The adsorption of biological molecules from the endolysosomal environment after longer incubation times is expected and may indicate the release of the 2-NAT from the gold nanostructures after some time.[68] Because the function of endolysosomes and phagosomes is the breakdown of organic molecules, also the thiol linkage of the 2-NAT reporter to the gold nanoparticle surface can be cleaved and would result in its release.[69] The properties of the reporter molecules over time in the two-photon experiments, as well as the possibilities to use the SEHRS probes as labeled nanoprobes of the cellular environment, must be further extended in future studies. Specifically, further investigations with model systems will be needed to better understand the vibrational fingerprint of SEHRS-based nanosensors and their interactions with different biomolecules in more detail.

4 | CONCLUSIONS

SEHRS spectra of different molecules were obtained with citrate-stabilized silver and gold nanoparticles using picosecond laser pulses at a wavelength of 1,550 nm and under conditions that are suitable to carry out microscopic experiments with biological samples, inside and outside of cells. The characteristic spectra of the molecules 2-NAT, *p*ATP, and CV as potential reporters for SEHRS labels and of the two antidepressant drugs desipramine and imipramine are qualitatively in good agreement with other off-resonance SEHRS data that were obtained from the same molecules previously.[21,36,39] The SEHRS spectrum of *p*NTP has not been reported so far, and the bands in the spectrum could be assigned based on the well-known SERS spectrum of the molecule. Discrimination between the spectra of *p*ATP and *p*NTP in principle also enables the observation of important reactions involving the two molecules,[56] and thereby other applications, in particular in catalysis research.

In spite of the obvious trade-off regarding biocompatible excitation intensities, the bottleneck concerning combination of both highly efficient excitation at 1,550 nm and HRS detection in one bio-suitable objective, and sufficient signal-to-noise ratio, all different types of nanoparticles yielded SEHRS signals that allowed discrimination of the reporter 2-NAT and of signals from the endolysosomal environment in the macrophage cells here. After longer incubation times with the SEHRS labels, the occurrence of spectral bands of molecules in the cells, including lipids and proteins, increases, suggesting the replacement of the 2-NAT reporter in the extreme environment of the endolysosome.

The SEHRS spectra obtained in living cells at this long wavelength—compared with those of previous reports[19,21]—indicate that the plasmonic properties of the nanoparticle aggregates during their processing by the cells are suited for the enhancement by both gold and silver nanostructures. The respective role of the electromagnetic enhancement of the excitation and the hyper-Raman fields[34] and the formation of nanoaggregates in the biosystem[61] will be elucidated further in order to optimize the plasmonic nanostructures for this excitation wavelength and to harness SEHRS for the acquisition of vibrational information from the biomolecules in living cells.

ACKNOWLEDGEMENTS

We thank Alexander Lang for making available the Onefive Katana laser. We thank Dr. Harald Kneipp and Dr. Daniela Drescher for valuable discussions. Funding by ERC Grant No. 259432 MULTIBIOPHOT to J. K. and by Deutsche Forschungsgemeinschaft (DFG) (GSC 1013 SALSA) is gratefully acknowledged. Further, Z. H. and V. Z. acknowledge funding through DFG GSC 1013 SALSA by a Julia Lermontova Postdoctoral Fellowship and a doctoral fellowship, respectively. F. M. acknowledges a Chemiefonds Fellowship (Fonds der Chemischen Industrie). Open access funding enabled and organized by Projekt DEAL.

CONFLICT OF INTEREST

The authors declare no competing financial interest.

ORCID

Janina Kneipp https://orcid.org/0000-0001-8542-6331

REFERENCES

[1] D. L. Jeanmaire, R. P. Van Duyne, *J. Electroanal. Chem. Interfacial Electrochem.* **1977**, *84*, 1.
[2] P. L. Stiles, J. A. Dieringer, N. C. Shah, R. P. V. Duyne, *Annu. Rev. Anal. Chem.* **2008**, *1*, 601.
[3] M. G. Albrecht, J. A. Creighton, *J. Am. Chem. Soc.* **1977**, *99*, 5215.
[4] J. Kneipp, *ACS Nano* **2017**, *11*, 1136.
[5] A. Matschulat, D. Drescher, J. Kneipp, *ACS Nano* **2010**, *4*, 3259.
[6] H. K. Yuan, Y. Liu, A. M. Fales, Y. L. Li, J. Liu, T. Vo-Dinh, *Anal. Chem.* **2013**, *85*, 208.
[7] S. Schlücker, B. Küstner, A. Punge, R. Bonfig, A. Marx, P. Ströbel, *J. Raman Spectrosc.* **2006**, *37*, 719.
[8] C. Fasolato, S. Giantulli, I. Silvestri, F. Mazzarda, Y. Toumia, F. Ripanti, F. Mura, F. Luongo, F. Costantini, F. Bordi, P. Postorino, F. Domenici, *Nanoscale* **2016**, *8*, 17304.
[9] C. L. Zavaleta, B. R. Smith, I. Walton, W. Doering, G. Davis, B. Shojaei, M. J. Natan, S. S. Gambhir, *Proc. Natl. Acad. Sci. U. S. A.* **2009**, *106*, 13511.
[10] S. Charan, F.-C. Chien, N. Singh, C.-W. Kuo, P. Chen, *Chem. A Eur. J.* **2011**, *17*, 5165.
[11] A. Michota, J. Bukowska, *J. Raman Spectrosc.* **2003**, *34*, 21.
[12] W. K. Wang, L. M. Zhang, L. Li, Y. Tian, *Anal. Chem.* **2016**, *88*, 9518.
[13] B. Gardner, N. Stone, P. Matousek, *Faraday Discuss.* **2016**, *187*, 329.
[14] B. Kang, M. M. Afifi, L. A. Austin, M. A. El-Sayed, *ACS Nano* **2013**, *7*, 7420.
[15] V. Zivanovic, S. Seifert, D. Drescher, P. Schrade, S. Werner, P. Guttmann, G. P. Szekeres, S. Bachmann, G. Schneider, C. Arenz, J. Kneipp, *ACS Nano* **2019**, *13*, 9363.
[16] A. V. Baranov, Y. S. Bobovich, *JETP Lett.* **1982**, *36*, 339.
[17] D. V. Murphy, K. U. Vonraben, R. K. Chang, P. B. Dorain, *Chem. Phys. Lett.* **1982**, *85*, 43.
[18] J. T. Golab, J. R. Sprague, K. T. Carron, G. C. Schatz, R. P. V. Duyne, *J. Chem. Phys.* **1988**, *88*, 7942.
[19] J. Kneipp, H. Kneipp, K. Kneipp, *Proc. Natl. Acad. Sci.* **2006**, *103*, 17149.
[20] J. Kneipp, H. Kneipp, B. Wittig, K. Kneipp, *Nano Lett.* **2007**, *7*, 2819.
[21] Z. Heiner, M. Gühlke, V. Živanović, F. Madzharova, J. Kneipp, *Nanoscale* **2017**, *9*, 8024.
[22] Y. Kitahama, H. Hayashi, T. Itoh, Y. Ozaki, *Analyst* **2017**, *142*, 3967.
[23] F. Madzharova, Á. Nodar, V. Živanović, M. R. S. Huang, C. T. Koch, R. Esteban, J. Aizpurua, J. Kneipp, *Adv. Funct. Mater.* **2019**, *29*, 1904289.
[24] V. N. Denisov, B. N. Mavrin, V. B. Podobedov, *Phys. Rep.* **1987**, *151*, 1.
[25] L. D. Ziegler, *J. Raman Spectrosc.* **1990**, *21*, 769.
[26] W. H. Yang, J. Hulteen, G. C. Schatz, R. P. V. Duyne, *J. Chem. Phys.* **1996**, *104*, 4313.
[27] J. C. Hulteen, M. A. Young, R. P. Van Duyne, *Langmuir* **2006**, *22*, 10354.
[28] N. Valley, L. Jensen, J. Autschbach, G. C. Schatz, *J. Chem. Phys.* **2010**, *133*, 054103.
[29] M. Gühlke, Z. Heiner, J. Kneipp, *Phys. Chem. Chem. Phys.* **2015**, *17*, 26093.
[30] M. J. Trujillo, J. P. Camden, *ACS Omega* **2018**, *3*, 6660.
[31] C. I. Wen, H. Hiramatsu, *J. Raman Spectrosc.* **2020**, *51*, 274.
[32] K. Kneipp, H. Kneipp, F. Seifert, *Chem. Phys. Lett.* **1995**, *233*, 519.
[33] T. Itoh, Y. Ozaki, H. Yoshikawa, T. Ihama, H. Masuhara, *Appl. Phys. Lett.* **2006**, *88*, 084102.
[34] F. Madzharova, Z. Heiner, J. Simke, S. Selve, J. Kneipp, *J. Phys. Chem. C* **2018**, *122*, 2931.
[35] H. K. Turley, J. P. Camden, *Chem. Commun.* **2014**, *50*, 1472.
[36] H. K. Turley, Z. Hu, D. W. Silverstein, D. A. Cooper, L. Jensen, J. P. Camden, *J. Phys. Chem. C* **2016**, *120*, 20936.
[37] G. Frens, *Nat. Phys. Sci.* **1973**, *241*, 20.
[38] P. C. Lee, D. Meisel, *J. Phys. Chem.* **1982**, *86*, 3391.
[39] F. Madzharova, Z. Heiner, J. Kneipp, *J. Phys. Chem. C* **2020**, *124*, 6233.
[40] Z.-M. Zhang, S. Chen, Y.-Z. Liang, Z.-X. Liu, Q.-M. Zhang, L.-X. Ding, F. Ye, H. Zhou, *J. Raman Spectrosc.* **2010**, *41*, 659.
[41] R. A. Alvarez-Puebla, D. S. Dos Santos Jr, R. F. Aroca, *Analyst* **2004**, *129*, 1251.
[42] A. Jaworska, K. Malek, *J. Colloid Interface Sci.* **2014**, *431*, 117.
[43] V. Živanović, F. Madzharova, Z. Heiner, C. Arenz, J. Kneipp, *J. Phys. Chem. C* **2017**, *121*, 22958.
[44] H. B. Lueck, D. C. Daniel, J. L. McHale, *J. Raman Spectrosc.* **1993**, *24*, 363.
[45] R. E. Weston, A. Tsukamoto, N. N. Lichtin, *Spectrochim. Acta A* **1966**, *22*, 433.
[46] M. Osawa, N. Matsuda, K. Yoshii, I. Uchida, *J. Phys. Chem.* **1994**, *98*, 12702.
[47] D.-Y. Wu, X.-M. Liu, Y.-F. Huang, B. Ren, X. Xu, Z.-Q. Tian, *J. Phys. Chem. C* **2009**, *113*, 18212.
[48] B. O. Skadtchenko, R. Aroca, *Spectrochim. Acta, Part A* **2001**, *57*, 1009.
[49] Y. Ling, W. C. Xie, G. K. Liu, R. W. Yan, D. Y. Wu, J. Tang, *Sci. Rep.* **2016**, *6*, 31981.
[50] M. Gühlke, Z. Heiner, J. Kneipp, *Phys. Chem. Chem. Phys.* **2016**, *18*, 14228.
[51] N. R. Agarwal, A. Lucotti, M. Tommasini, F. Neri, S. Trusso, P. M. Ossi, *Sens. Actuators B* **2016**, *237*, 545.
[52] B. Dong, Y. Fang, L. Xia, H. Xu, M. Sun, *J. Raman Spectrosc.* **2011**, *42*, 1205.
[53] P. E. Laibinis, M. A. Fox, J. P. Folkers, G. M. Whitesides, *Langmuir* **1991**, *7*, 3167.
[54] J. C. Love, L. A. Estroff, J. K. Kriebel, R. G. Nuzzo, G. M. Whitesides, *Chem. Rev.* **2005**, *105*, 1103.
[55] J.-H. Kim, J.-S. Kim, H. Choi, S.-M. Lee, B.-H. Jun, K.-N. Yu, E. Kuk, Y.-K. Kim, D. H. Jeong, M.-H. Cho, Y.-S. Lee, *Anal. Chem.* **2006**, *78*, 6967.
[56] V. Joseph, C. Engelbrekt, J. Zhang, U. Gernert, J. Ulstrup, J. Kneipp, *Angew. Chem. Int. Ed.* **2012**, *51*, 7592.
[57] F. Madzharova, Z. Heiner, J. Kneipp, *J. Phys. Chem. C* **2017**, *121*, 1235.
[58] F. Madzharova, Z. Heiner, M. Gühlke, J. Kneipp, *J. Phys. Chem. C* **2016**, *120*, 15415.
[59] D. Drescher, P. Guttmann, T. Büchner, S. Werner, G. Laube, A. Hornemann, B. Tarek, G. Schneider, J. Kneipp, *Nanoscale* **2013**, *5*, 9193.
[60] T. Büchner, D. Drescher, H. Traub, P. Schrade, S. Bachmann, N. Jakubowski, J. Kneipp, *Anal. Bioanal. Chem.* **2014**, *406*, 7003.

[61] D. Drescher, T. Büchner, P. Guttmann, S. Werner, G. Schneider, J. Kneipp, *Nanoscale Adv.* **2019**, *1*, 2937.
[62] J. Kneipp, H. Kneipp, M. McLaughlin, D. Brown, K. Kneipp, *Nano Lett.* **2006**, *6*, 2225.
[63] Z. Movasaghi, S. Rehman, I. U. Rehman, *Appl. Spectros. Rev.* **2007**, *42*, 493.
[64] K. Czamara, K. Majzner, M. Z. Pacia, K. Kochan, A. Kaczor, M. Baranska, *J. Raman Spectrosc.* **2015**, *46*, 4.
[65] A. C. S. Talari, Z. Movasaghi, S. Rehman, I. Rehman, *Appl. Spectros. Rev.* **2015**, *50*, 46.
[66] N. Kuhar, S. Sil, T. Verma, S. Umapathy, *RSC Adv.* **2018**, *8*, 25888.
[67] G. P. Szekeres, J. Kneipp, *Analyst* **2018**, *143*, 6061.
[68] M. Borzenkov, G. Chirico, L. D'Alfonso, L. Sironi, M. Collini, E. Cabrini, G. Dacarro, C. Milanese, P. Pallavicini, A. Taglietti, C. Bernhard, F. Denat, *Langmuir* **2015**, *31*, 8081.
[69] K. J. F. Carnevale, G. F. Strouse, *Bioconjug. Chem.* **2018**, *29*, 3429.

SUPPORTING INFORMATION

Additional supporting information may be found online in the Supporting Information section at the end of this article.

How to cite this article: Heiner Z, Madzharova F, Živanović V, Kneipp J. Bio-probing with nonresonant surface-enhanced hyper-Raman scattering excited at 1,550 nm. *J Raman Spectrosc*. 2020;1–10. https://doi.org/10.1002/jrs.5965